Available online at www.sciencedirect.com
ScienceDirect
Journal of Magnetic Resonance 184 (2007) 101–107
JMR Journal of Magnetic Resonance
www.elsevier.com/locate/jmr

Enhanced Overhauser contrast in proton–electron double-resonance imaging of the formation of an alginate hydrogel

Wilson Barros Jr. *, M. Engelsberg

Departamento de Física, Universidade Federal de Pernambuco, Av. Prof. Luís Freire s/n. 50670-901, Recife, PE, Brazil

Received 26 March 2006; revised 21 September 2006
Available online 13 October 2006

Abstract

Proton–electron double-resonance imaging (PEDRI) was recently employed to monitor the process of formation of a calcium alginate hydrogel at a field of 16 mT. Here, under the same experimental conditions, images obtained through this technique are compared to images obtained by conventional T_2-weighted method. The results confirm that the image contrast obtained using PEDRI, thanks to the Overhauser effect, exhibits an improved sensitivity with respect to changes in water mobility as previously suggested in the literature. Furthermore, by increasing the echo time interval for the T_2-weighted images, important features of the gelling dynamics obtained via PEDRI could not be reproduced.

Keywords: Overhauser; PEDRI; Alginate; MRI; T_2 contrast; Gelling process

1. Introduction

The use of magnetic resonance imaging (MRI) in material science applications has become widespread over the years [1–3]. By looking at the image profiles obtained through properly designed experimental arrangements it is possible to assess aspects of the structure, the underlying mechanisms of transport and chemical kinetics of many interesting processes [1,2,4,5]. In particular, the possibility of monitoring these processes with spatial resolution constitutes a unique advantage of MRI over methods where only global temporal dynamics can be extracted.

The MRI technique exhibits an inherently low signal-to-noise efficiency. Usually, despite the high costs involved, signal-enhancement is generated by utilizing high polarizing fields powered by super-conducting magnets. However, there are ways of improving the signal-to-noise ratio without necessarily increasing the polarizing field. For instance, a dynamic nuclear polarization (DNP) [6] method based on the Overhauser effect [7] can produce good quality MR images at low polarizing magnetic fields [8]. The method consists of irradiating an electron paramagnetic resonance (EPR) line of a free radical in solution and, via cross-relaxation processes between the unpaired electrons and the coupled solvent nuclei, induce an increase in the nuclear spin polarization. The signal enhancement is a function of the ratio $\gamma_e/\gamma_p = 660$ of the magnetogyric factors of two types of spins involved in the process. Its large value justifies the use electron–proton polarization transfer for signal enhancement. The potential difference in the Overhauser contrast when compared to conventional imaging techniques is related to the role of the free radical as an active factor in the polarization transfer. Recently, in addition to the signal-to-noise ratio enhancement, it has been shown that the imaging contrast produced via Overhauser

* Corresponding author. Present address: Vanderbilt University Institute of Imaging Science (VUIIS), Vanderbilt University Medical Center, R-1302 Medical Center North, Nashville, TN 37232-2310, USA. Fax: +1 615 322 0734.
E-mail address: wilson.barros@vanderbilt.edu (W. Barros Jr.).

1090-7807/$ - see front matter © 2006 Elsevier Inc. All rights reserved.
doi:10.1016/j.jmr.2006.09.020

effect can be very sensitive to mobility changes of the water molecules [9–12].

Although gels exhibit solid-like characteristics on a macroscopic level, microscopically they behave in a liquid-like fashion suitable for MRI investigation. Indeed, a considerable variation in water mobility is expected during the formation of gel systems. In particular, polysaccharides such as sodium alginate are especially interesting for their ability to form, with divalent cations such as calcium, a lattice gel of cross-linked chains that provides a biologically mild environment for immobilization of living cells, implants, and for drug delivery [13]. Although high field T_2-weighted images [14] indicate reduced mobility-sensitivity for the same type of gels studied here, the T_2 relaxation times as well as the reaction rates that determine the sharpness of the reaction-front change appreciably as a function of the alginate unitary constituent fractions. Thus, to conduct experiments on the same gel system under the same conditions turns out to be vital for a reliable comparison between different imaging modalities.

In order to confirm the enhanced mobility-contrast sensitivity generated via the Overhauser effect, we compare images of the formation process of alginate hydrogels [12] obtained under the same experimental conditions by a technique named proton–electron double-resonance imaging [15] (PEDRI) and by conventional T_2-weighted imaging. For the latter method, images with increasing values of the spin-echo time TE were recorded in an attempt to reproduce the same contrast-sensitivity of the images obtained by PEDRI. Finally, as a way to quantify the range of sensitivity of the mobility contrast obtained via the Overhauser effect, PEDRI signal amplitudes of homogeneously prepared samples of calcium alginate gels with different concentrations of initial sodium alginate were acquired as a function of calcium concentration.

2. Theory

The Overhauser contrast observed utilizing the PEDRI method depends upon several factors which are different from those prevailing in conventional MRI. (A more complete treatment [9,10] can be found elsewhere and here only the most basic results will be presented.) The PEDRI technique is performed by dissolving a small amount of a free radical (typically a few mM) into a water solution and then transferring polarization, via a saturating EPR pulse, from the unpaired electrons in the free radical to the ^{1}H nuclei present in the water molecules. Typically the electron–proton DNP requires low polarizing magnetic fields since water-soluble systems may become opaque for high-frequency EPR irradiation. (Field cycling techniques can be utilized to circumvent this limitation [16].)

In a steady state regime, the signal enhancement E generated by saturating the electronic transition S and detecting the water protons transition I is given by [9]

$$E = \frac{\langle I_z \rangle}{I_0} = 1 - \rho f \frac{|\gamma_e|}{\gamma_p} s, \tag{1}$$

where $\langle I_z \rangle$ is the average nuclear magnetization generated by the polarization transfer and I_0 is the equilibrium nuclear magnetization produced in the presence of the polarizing field. The parameter f is the leakage factor, ρ is the coupling factor, s denotes the degree of saturation for the electronic transition, and finally γ_e and γ_p are, respectively, the magnetogyric factor of the electrons unpaired in the free radical and that of the protons present in the water molecules.

The leakage factor f in Eq. (1) accounts for the loss in the Overhauser enhancement caused by spin–lattice relaxation of nuclei within the solvent molecules via proton–proton dipolar couplings. More explicitly, f is given by

$$f = 1 - \frac{T_1}{T_{10}} = \frac{kCT_{10}}{1 + kCT_{10}}. \tag{2}$$

Here, T_1 denotes the NMR spin–lattice relaxation time of the water protons of the free radical solution. The protons relaxation time in the absence of the free radical in given by T_{10}. The concentration of free radical is given by C and k denotes the relaxivity constant. f indicates that, in order to detect an appreciable enhancement, the electron spins in the free radical must provide the dominant relaxation mechanism for the NMR nuclei.

The coupling factor ρ is dependent upon the nature of the proton–electron interaction and the magnetic field strength. At low free radical concentration, dipolar interactions are responsible for the electron–proton cross-relaxation process. Low polarizing fields, as in the experiments described here, make the inverse of the electronic Larmor frequency larger than the characteristic correlation time of molecular motion (extreme narrowing limit). These combined effects give $\rho = 1/2$.

The s factor is a function of irradiation power and the electron spin relaxation times. Steady-state on-resonance irradiation yields

$$s = \frac{(S_0 - \langle S_z \rangle)}{S_0} = \frac{\gamma_e^2 B_1^2 T_{1e} T_{2e}}{1 + \gamma_e^2 B_1^2 T_{1e} T_{2e}}, \tag{3}$$

where S_0 is the equilibrium zeeman magnetization for the electrons and $\langle S_z \rangle$ is the electronic polarization under the saturation irradiation. B_1 is the amplitude of the oscillating magnetic field used to saturate the electronic transition, T_{1e} and T_{2e} are the electron spin–lattice and spin–spin relaxation times, respectively. Via these relaxation times a relation between the mobility of the radical and the saturating parameter is established. If the extreme narrowing condition does not hold, e.g., when the molecular motion is not fast enough, it is necessary to introduce correlation functions for the electron–proton and proton–proton dipole–dipole interaction [10]. Moreover, if the steady-state regime is not valid, i.e., if T_1 is larger than the electronic irradiation interval a correcting term [10] needs to be included in Eq. (1). In fact, a detailed analysis and evaluation of the abso-

lute value of the Overhauser signal enhancement seems not to be necessary for experiments as those described here where only relative changes in the image profiles are important for determining the associated contrast.

3. Experiments

The experimental setup for observing the process of gelling of a sodium alginate solution in the presence of calcium ions is shown on Fig. 1. The arrangement displays two nested concentric reservoirs: a dialysis membrane (internal reservoir) of 14.5 mm (i.d.) and 30 mm height containing a 3% (w/v) aqueous solution of sodium alginate (The membrane is impermeable to alginate macromolecules but permeable to other ions); and a cylindrical glass vial (outer reservoir) with 25 mm (i.d.) and also a 30 mm height containing a 60 mM aqueous solution of $CaCl_2$. In both reservoirs, a 2.5 mM concentration of the triaryl methyl (TAM) free radical OX063 [17] was dissolved.

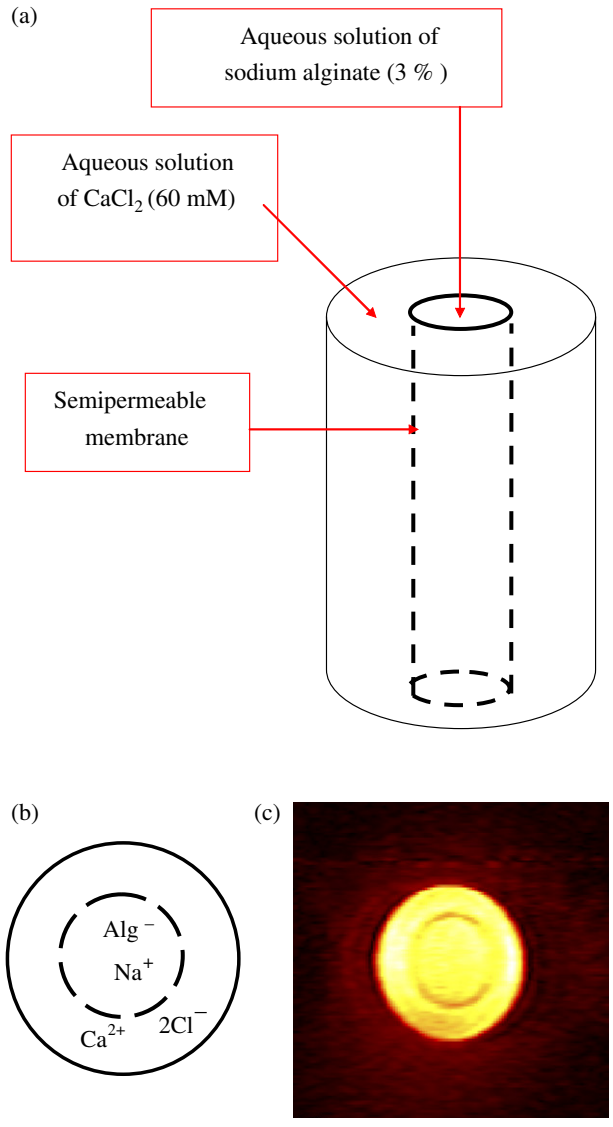

Fig. 1. Description of the experimental setup designed to monitor the calcium alginate formation: (a) A semipermeable dialysis membrane containing a 3% (w/v) sodium alginate solution is immersed into a glass vial containing 60 mM of $CaCl_2$ forming two concentric reservoirs; (b) top view of the arrangement depicting the cations and anions involved in the process; (c) an axial slice of a typical PEDRI (see Fig. 2) image of the experimental arrangement showing the two regions at an early stage of the gelling process (TE = 30 ms, 128×64 matrix, 0.38 mm in-plane resolution, four averages, and EPR irradiation interval $t_{EPR} = 500$ ms with 10 W power).

The measurements were conducted in a home-built MRI scanner able to generate a polarizing field of 16 mT corresponding to a resonance frequency of 680 kHz for the ^1H nuclei. The DNP technique was performed by saturating the single-line transition of the unpaired electron spins of the free radical using a birdcage resonator of 30 mm (i.d.) inserted into a solenoid receiver coil tuned to detect the ^1H NMR signal of the water molecules. The OX063 single-line EPR transition [18], corresponding in a field of 16 mT to a frequency of 447 MHz, was saturated by a 10 W amplifier during a period $t_{EPR} = 500$ ms. An Overhauser enhancement of a factor of 50 was observed for a test sample containing 2.5 mM of OX063 radical dissolved in water. Following the saturation period, a conventional spin-warp protocol was used to acquire an image (see Fig. 2). The T_2-weighted images were performed under the same experimental conditions but turning the EPR irradiation off during t_{EPR}. Unless otherwise mentioned the spin-echo interval TE used was 30 ms and the imaging gradients were adjusted in order to produce an in-plane pixel size of 0.645 mm with a slice thickness of 20 mm. Each image took 7.7 min for a 128×64 matrix with 4 averages.

The cycling time of the PEDRI sequence, TR = 1.8 s, was chosen so that it corresponds to approximately $3T_{10}$. Here $T_{10} = 600$ ms denotes the spin–lattice relaxation time of an aqueous 3% (w/v) solution of alginate containing 2.5 mM of OX063 radical prior to gelation, when no calcium ions are present. This choice of TR substantially reduces the effect of spin–lattice relaxation on image contrast at the beginning of the process. As the gelation progresses slowing down molecular motion, regions of the sample with reduced water mobility could relax at a substantially slower rate than $1/T_{10}$ therefore introducing some T_1 contrast. However, since we will be comparing signal amplitudes with and without EPR irradiation in the same system under identical conditions, the effect of T_1 on overall image contrast will be present in both cases with equal strength.

Finally, a set of uniform sodium alginate aqueous solutions with concentrations varying from 2% to 4% (w/v) was prepared including 2.5 mM of OX063 radical. Homogeneous calcium alginate gels [19] with different concentrations of Ca^{2+} were prepared for each of the initial sodium alginate solution sets. Images of each gel sample were obtained at 16 mT using the PEDRI sequence described in Fig. 2. This experiment involved the same arrangement of two concentric reservoirs depicted in Fig. 1 but with a glass partition substituting for the dialysis membrane. The outer reservoir contained a 2.5 mM

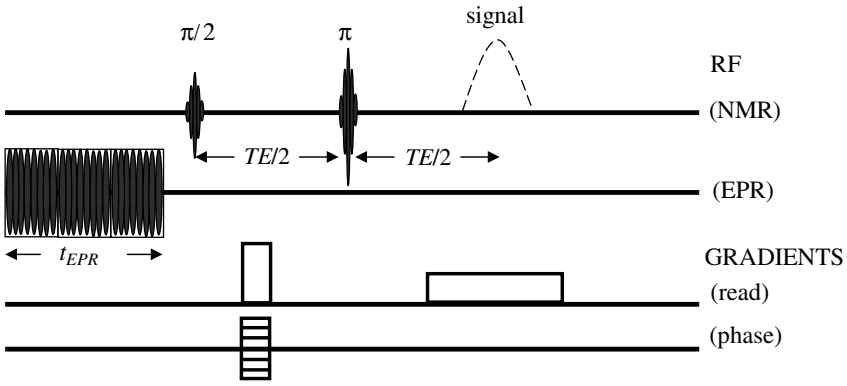

Fig. 2. Pulse diagram of the PEDRI sequence. It consists of a conventional spin-warp imaging protocol that includes an EPR saturation interval t_{EPR} (The pulse interval lengths are not in scale).

concentration of radical dissolved in an aqueous solution of 60 mM of $CaCl_2$. Its signal amplitude was assigned the value 255 that was used as a reference for the Overhauser enhancement.

4. Results and discussion

Fig. 3 shows axial image slices of the calcium alginate gelling process as a function of the dialysis time T during which the calcium cations cross the semi-permeable membrane and react with the sodium alginate. The decay in the signal amplitude is caused by changes in water mobility generated by the binding of the calcium ions to different pieces of the polymer forming the cross-linked network. Each PEDRI acquisition (images depicted on the left column of the panel) is followed by another acquisition with the electronic irradiation off (images depicted on the right column). Looking at the first ($T = 15$ and 23 min) and the last ($T > 48$ h) pairs of images, there is apparently as much detail present in the PEDRI images as in the conventional T_2-weighted images. However, the images from $T = 60$ to 278 min show a slightly different dynamics. The PEDRI images exhibit two main features: the first one is a sharp decay in the signal as the gelling reaction takes place (see, for instance, the vertical arrow for $T =$ 120 min). The second feature is a decay of the signal at the center of the image which occurs simultaneously with the reaction-front progression (see, for instance, the horizontal arrow for $T = 120$ min). Both features are important for the quantitative description of the gelling process [4]. To better appreciate the latter effect, Fig. 4 shows horizontally taken radial profiles of the region inside the dialysis membrane as the reaction takes place. The amplitude assigned to the signal from the outer reservoir, not shown in the figure, was 255. For conventional T_2-weighted images (right column), with a TE = 30 ms, the T_2 contrast is enough to observe the reaction-front (refer to the vertical arrow for $T = 128$ min) but clearly insufficient to catch the signal decay at the image center (refer to the arrow depicted horizontally for $T = 128$ min). The images using the T_2-weighted method do not show any pronounced decay even at the extreme case of 48 h after the dialysis started.

In conventional high-field MRI, contrast appears to be determined by the pronounced difference in spin–spin relaxation time between free sodium alginate solution and calcium alginate gel [14]. In order to take advantage of this difference and optimize contrast the echo-time TE must be increased. Fig. 5 shows axial image slices obtained in a field of 16 mT using the sequence described on Fig. 2 with the EPR irradiation off during $t_{SE} = 500$ ms. The spin-echo time TE for the images from (a) to (e) was varied from 30 ms up to 200 ms. The image (a) corresponds to a dialysis time $T = 300$ min and the following images were recorded at later intervals as indicated in the figures. On the right side of both (a) and (e), the respective PEDRI images (TE = 30 ms) were used as reference for comparison. As TE is changed, the T_2 contrast becomes observable and the regions where the gel has already reacted turn darker in the images (vertical arrows for (a) and (d)). For $T > 270$ min the reaction process is almost completed and the changes in the images from (c) to (e) are expected to result only from changes in the T_2-weighting and not from additional reaction. Surprisingly, for the interval of TE values covered by this experiment, the signal at the center of the membrane maintains its brightness up to TE = 200 ms (see the horizontal arrow in the figure (e)). However, the signal-to-noise gets worse as TE increases and, for image (e), it is likely that the signal at the center of image is considerably affected by noise. Although a quantitative evaluation is challenging, the image gives clear evidence that the contrast generated by T_2-weighted method proves inefficient in reproducing the PEDRI profiles.

PEDRI signal amplitude not only is a function of calcium concentration in the gel but also depends on the initial sodium alginate concentration. Fig. 6 shows an experiment where the PEDRI signal amplitudes of homogeneous calcium alginate samples, prepared as described in reference [19], are plotted as a function of the Ca^{2+} concentration. The images were produced using the sequence described in Fig. 2. Each image amplitude was

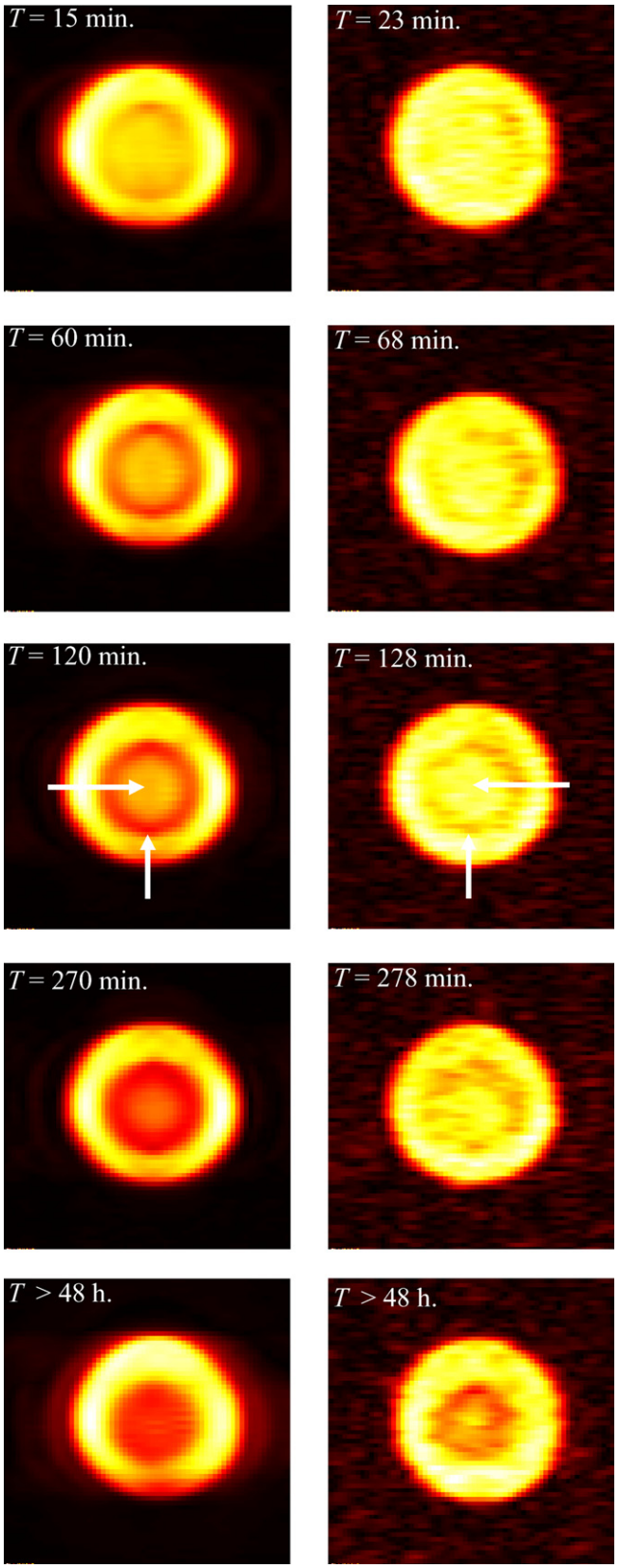

Fig. 3. Axial slice images of the calcium alginate formation as a function of the dialysis time T. The left column shows PEDRI images acquired using TE = 30 ms, t_{EPR} = 500 ms (10 W of irradiation power), and an in-plane pixel size of 0.645 mm. The right column shows images acquired at the same experimental conditions but with the EPR power off.

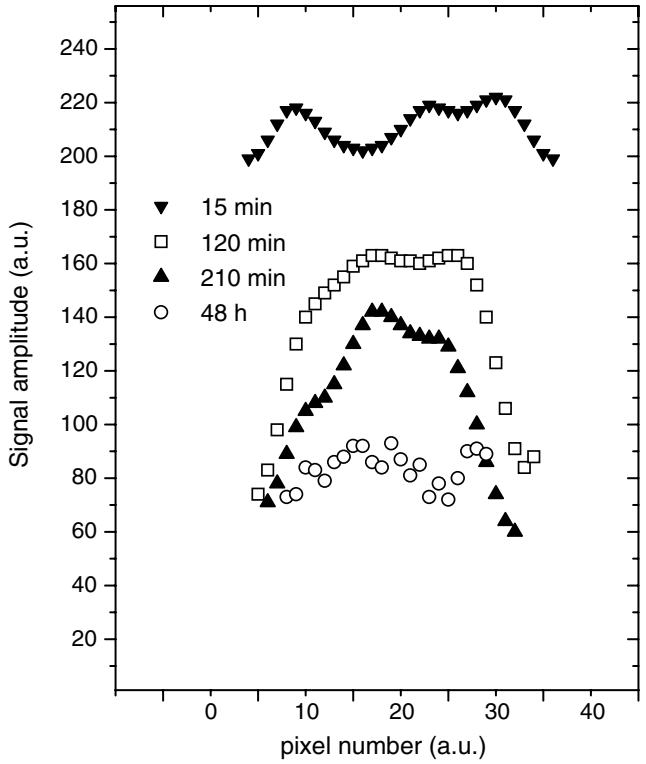

Fig. 4. Radial profiles taken horizontally from the PEDRI experiments of Fig. 3 for dialysis times T = 15, 120, 210 min and 48 h. The profiles depict the region inside the dialysis membrane. The PEDRI signal amplitude is normalized relative to an outside reservoir, not shown in the profile, containing $CaCl_2$ (60 mM) and OX063 (2.5 mM) free radical.

normalized by the signal amplitude of a reference sample containing a 60 mM aqueous solution of $CaCl_2$ with 2.5 mM of OX063 radical dissolved. The three curves represent samples with different initial sodium alginate concentrations and are useful to quantitatively demonstrate the sensitivity range of the Overhauser enhancement to changes in mobility caused by the increase in calcium concentration [20]. The samples containing 2% (w/v) and 3% (w/v) initial sodium alginate are already viscous enough to show a decrease in signal amplitude when compared to the reference sample. This decay is even more dramatic for the sample containing 4% (w/v) of initial sodium alginate. The profiles of the 2% (w/v) and 3% (w/v) initial sodium alginate solutions show similar ratio between the maximum and the minimum signal amplitude, of approximately a factor of 4. For the slightly more concentrated 4% (w/v) sodium alginate sample, the ratio decreased by a factor of 2. The contrast sensitivity to mobility changes turns out to be particularly important at low concentrations of the initial sodium alginate solution where a high sensitivity in the PEDRI signal can be observed as a function of calcium concentrations up to 10 mM. This may not constitute a limitation for PEDRI since previous results [11] indicate that the contrast-sensitivity can be tuned according to the characteristics of the system being investigated.

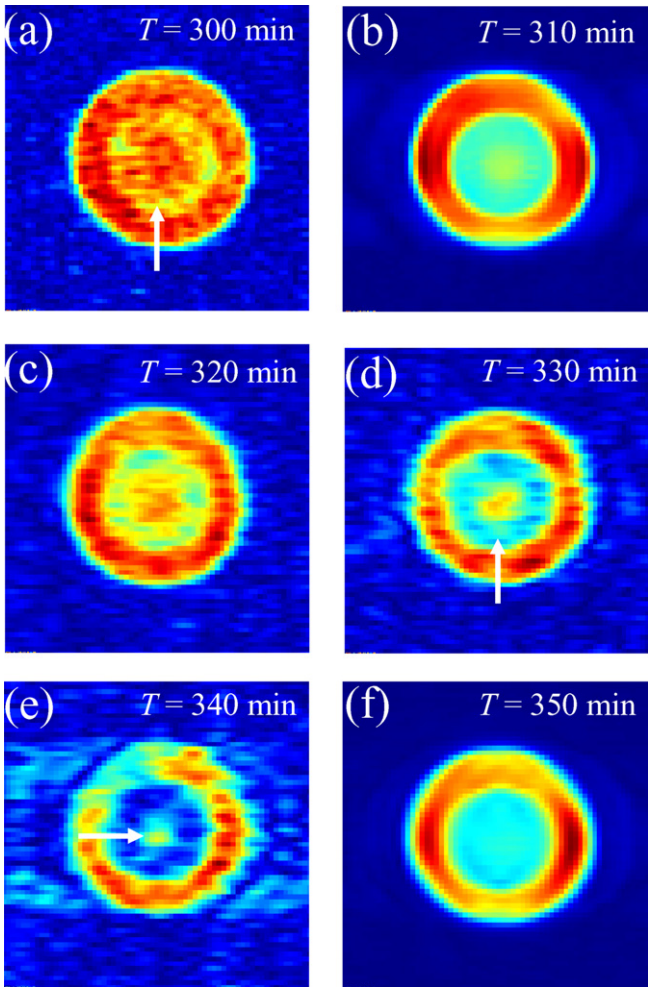

Fig. 5. Axial slice images of the same calcium alginate formation shown in Fig. 3 as a function of the dialysis time T. The images (a), (c), (d) and (e) were obtained via the sequence in Fig. 2 with EPR irradiation off. The images were recorded using different values of TE: (a) 30 ms, (c) 60 ms, (d) 100 ms, and (e) 200 ms. As a reference for comparison, on the right column, the images (b) and (f) are PEDRI images recorded using TE = 30 ms and the same in-plane resolution of Fig. 3.

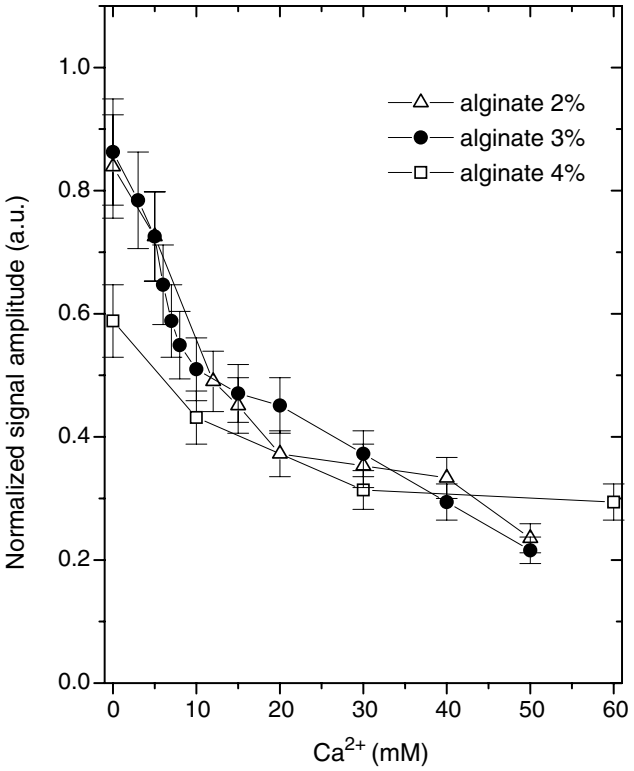

Fig. 6. PEDRI signal amplitude as a function of the Ca^{2+} concentration for homogeneously prepared alginate gels containing 2.5 mM of OX063 radical. The symbols represent different concentrations of the initial sodium alginate (error bars indicate 10% of uncertainty). The data were obtained using the sequence described in Fig. 2 with TE = 30 ms and t_{EPR} = 500 ms with 10 W of irradiation power (The solid lines are guide for the eyes).

5. Conclusions

By monitoring the formation of a calcium alginate gel at 16 mT We confirmed that, under the same experimental conditions, the PEDRI method is more sensitive to changes in water mobility than conventional T_2-weighted imaging. In addition, by increasing the spin-echo time TE up to 200 ms in the T_2-weighted images, the mobility-contrast sensitivity associated to the water dynamics was inferior to that obtained using the PEDRI method.

To perform T_2-weighted images of the alginate formation process in a higher polarizing field would be very useful in order to alleviate the noise background present in the images acquired at 16 mT for long spin-echo intervals. Instead T_2 measurements (data not shown) were performed in a field of 7 T for the homogeneously prepared alginate samples of 3% (w/v) aqueous solution of sodium alginate as a function of the calcium concentration. The experiment corroborates the results obtained at low field for TE = 30 ms presented here and also those performed at 2 T with TE = 100 ms reported by Potter et al. [14].

Although recently developed bio-compatible free radicals providing narrow-line electronic transition and requiring lower saturating power are promising for in vivo studies [18,21], material science applications offer more flexibility in terms of sample size and non-invasiveness. Small samples permit more homogeneous excitation and larger signal enhancement can be accomplished by either performing the electronic-transition saturation during longer intervals or using higher irradiation power. It is worth mentioning the good quality of the images obtained without the EPR irradiation which are relative to a polarization field of only 16 mT. In addition, implementations including fast imaging protocols may allow for an improvement in the signal-to-noise per time. Likewise, resolution can be increased as well as more rapid reacting systems be probed.

Finally, we conclude that PEDRI may be a useful tool for studying spatio-temporal dynamics of dilute-solution reactions exhibiting changes in mobility especially at initial transition stages. The methodology offers potential accessibility to new effects using a magnet design and cost much more affordable.

Acknowledgments

We thank one of the reviewers for useful comments. This work was supported by Conselho Nacional de Desenvolvimento Científico e Tecnológico (Brazilian Agency).

References

[1] J.B. Miller, NMR imaging of materials, Prog. NMR Spectrosc. 33 (1998) 273–308.
[2] P.T. Callaghan, Principles of Nuclear Magnetic Resonance Microscopy, Claredon Press, Oxford, 1991.
[3] N. Nestle, K. Shet, D.J. Lurie, Proton electron double resonance imaging of free radical distribution in environmental science applications—first results and perspectives, Magn. Reson. Imaging 23 (2005) 183–189.
[4] W. Barros Jr., M. Engelsberg, Enhanced migration and ionic transport through membranes, Phys. Rev. E 67 (2003) 021905–021909.
[5] A.J. Sederman, M.D. Mantle, C. Buckley, L.F. Gladden, MRI technique for measurement of velocity vectors, acceleration, and autocorrelation functions in turbulent flow, J. Magn. Reson. 166 (2004) 182–189.
[6] C.P. Slichter, Principles of Magnetic Resonance, third enlarged and updated ed., Springer, New York, 1990.
[7] A.W. Overhauser, Polarization of nuclei in metals, Phys. Rev. 92 (1953) 411–412.
[8] K. Golman, I. Leunbach, J.S. Petersson, D. Holz, J. Overweg, Overhauser-enhanced MRI, Acad. Radiol. 9 (2002) 104–108.
[9] I. Nicholson, D.-J. Lurie, F.J.L. Robb, The application of proton–electron double-resonance imaging techniques to proton mobility studies, J. Magn. Reson. Ser. B 104 (1994) 250–255.
[10] P.L. de Sousa, R.E. de Souza, M. Engelsberg, L.A. Colnago, Mobility and free radical concentration effects in proton–electron double-resonance imaging, J. Magn. Reson. 135 (1998) 118–125.
[11] P.L. de Sousa, M. Engelsberg, M.A. Matos, L.A. Colnago, Measurements of water transport in a gel by Overhauser magnetic resonance imaging, Meas. Sci. Technol. 9 (1998) 1982–1988.
[12] W. Barros Jr., R.E. de Souza, M. Engelsberg, K. Golman, J.H. Ardenkjær-Larsen, Low field Overhauser images of the formation process of a hydrogel, Appl. Phys. Lett. 80 (2002) 160–162.
[13] S. Sakai, T. Ono, H. Ijima, K. Kawakami, In vitro and in vivo evaluation of alginate sol/gel synthesized aminopropyl-silicate/alginate membrane for bioartificial pancreas, Biomaterials 23 (2002) 4177.
[14] K. Potter, E.W. McFarland, Ion transport studies in calcium alginate gels by magnetic resonance microscopy, Solid State NMR 6 (1996) 323–331.
[15] D.J. Lurie, D.M. Bussel, L.H. Bell, J.R. Mallard, Proton–electron double magnetic resonance Imaging of free radical solutions, J. Magn. Reson. 76 (1988) 366–370.
[16] D.J. Lurie, G.R. Davies, M.A. Foster, J.M.S. Hutchison, Field cycling PEDRI imaging of free radicals with detection at 450 mT, Magn. Reson. Imaging 23 (2005) 175–181.
[17] Nycomed innovation AB, Malmö, Sweden (proprietary compound).
[18] J.H. Ardenkjær-Larsen, I. Laursen, I. Leunbach, et al., EPR and DNP properties of a certain novel single electron contrast agents intended for oximetrical imaging, J. Magn. Reson. 133 (1998) 1–12.
[19] K.I. Draget, K. Østgaard, O. Smidsrød, Homogeneous alginate gels: a technical approach, Carbohydr. Polym. 14 (1991) 159.
[20] W. Barros Jr., M. Engelsberg, Ionic transport, reaction kinetics, and gel formation. A low-field Overhauser magnetic resonance imaging study, J. Phys. Chem. A 106 (2002) 7251–7255.
[21] M.C. Krishna, S. English, K. Yamada, J. Yoo, R. Murugesan, et al., Overhauser enhanced magnetic resonance imaging for tumor oximetry: coregistration of tumor anatomy and tissue oxygen concentration, Proc. Natl. Acad. Sci. USA 99 (2002) 2216–2221.